Displaced orbits for nonideal flat solar sail in the circular restricted three-body problem with oblateness

Ming Song[1], Xingsuo He[2], Dongsheng He[1], YeHao Yan[1]
[1]Student, School of mechanics and civil & architecture, Northwestern polytechnical university, Xi'an ,China
email : astrosong09@yahoo.com

[2]Professor, School of mechanics and civil & architecture Northwestern polytechnical university Xi'an ,China

***Abstract*—We investigate displaced orbits of nonideal flat solar sail (NFS) in the circular restricted three-body problem with oblateness in the solar system and simulate the displaced orbits above the ecliptic plane by tracking a reference orbit. The model of NFS is introduced before establishing dynamic system. Linearization near the collinear equilibria of the system is applied. Linear quadratic regulator （LQR） is used to stabilize the nonlinear system. Displaced orbits above the ecliptic plane are simulated. The results reveal that the solar sail displaced orbits above the ecliptic plane is feasible and asymptotically stable.**

Keywords—Nonideal solar sail；Restricted three-body problem；Displaced orbits；Oblateness

I. INTRODUCTION

Solar sail, as one of the focusing subjects, has been studied during the first decade of the 21st century [1-5]. As we known, solar sail is consisted of polymeric thin film and light bracing structures [6]. Therefore, the mass of solar sail is defined as infinitesimal and the effects on celestial bodies are neglected in the orbital dynamics analysis. Solar sail uses sunlight to generate propulsion in space by reflecting solar photon flux from a large, mirror-like sail made of lightweight, highly reflective polyimide film material. In 2010 , the Interplanetary Kite-craft Accelerated by Radiation Of the Sun (IKAROS) made by JAXA (Japan Aerospace Exploration Agency) achieved the first success in the world [7]. After that, some new space missions using a solar sail were put forward, such as NanoSail-D [8], Cubesail [9], DeorbitSail [10] and Sunjammer [11]. Propulsion of solar sail comes from the solar radiation pressure, so the additional chemical propellant is not needed. For this reason, solar sail can be kept in NonKeplerian Orbits (NKOs) for a very long time. Displaced orbit, as one of the NKOs, has been investigated by many scientists. Simo [12] studied new families of NKOs in the Earth-Moon circular restricted three-body problem (CRTBP) using solar sailing and solar electric technology. Gong [13] used the coupled attitude-orbit dynamical model to analyze unstable displaced orbits. McInnes [14] put periodic impulses into the generation of connected three-body arcs at fixed positions. Ceriotti [15] presented doubly-symmetric, displaced eight-shaped orbits and these orbits could be used for continuous Earth polar coverage.

The restricted three-body problem (RTBP) has been considered a basic dynamic model ever since the scientists have studied the solar sail [16, 17]. The RTBP describes the motion of an infinitesimal mass, usually a satellite, solar sail or asteroid, moving under the gravitational effect of two finite masses, normally called primaries, which move in circular orbits about their center of mass under their mutual attraction [6]. Usually we do not take into account of the effect of the infinitesimal mass of the motion of the primaries. However, an absolute spherical celestial body is very rare in space, most of the planets are oblate. Sharma and Rao [18] investigated the locations of the five equilibrium points by considering the effect of oblateness of the more massive primary. Sharma [19, 20] discussed the existence of periodic orbits in the RTBP when the more massive primary was an oblate spheroid. Douskos [21, 22] focused on the equilibrium points and their stability in the Hill's problem with oblateness. Singh [23] analyzed the combined effects of perturbations, oblateness, and radiation of the primaries on the nonlinear stability of the Lagrange points. However, the above literatures did not take notice of the impacts of oblateness on solar sail orbits in RTBP. Therefore, the effects of the oblateness of the primaries should be included when we investigate the motion of the solar sail in the RTBP.

This paper is organized as follows. Section 2 gives an outline of the model of the NFS and the system in the circular restricted three-body problem, where the larger primary is an oblate spheroid. In Section 3, we investigate the collinear equilibrium points of the system. Then, in Section 4, linearization near the collinear Lagrange points is taken into account, and LQR is developed to stabilize the nonlinear system. The simulation is given in Section 5. The conclusions are discussed in Section 6.

II. Dynamic System

A. Non ideal solar sail model

According to McInnes [6]and Wright [24], we consider a simplified NFS, which only includes the effects of reflection and absorption. Figure 1.is the simplified model of NFS. $\boldsymbol{l}$ (vectors are expressed by black italicized letters in this article) is the unit vector of the incident light; $\boldsymbol{s}$ is the unit vector of the reflected light; $\boldsymbol{n}$ is the unit normal vector of the sail; $\boldsymbol{m}$ is the direction vector of the resultant solar radiation pressure force exerted on the sail; $\boldsymbol{t}$ is the unit vector of the transverse component of the total force. α is the incident angle; φ is the centerline angle and θ is the cone angle.

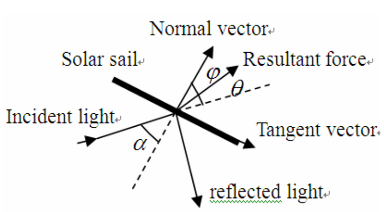

Figure 1. Simplified model of NFS

ρ_r is the reflection coefficient; ρ_a is the absorption coefficient; and the sum of these two coefficients is one. Then the acceleration of solar radiation pressure on NFS is derived [25, 26]

$$\boldsymbol{a} = \frac{PA_s}{m_s}\cos\alpha[2\rho_r\cos\alpha\boldsymbol{n} + (1-\rho_r)\boldsymbol{l}] \quad (1)$$

where P is the solar radiation pressure and inversely proportional to the square of the distance from the Sun. In this article, P is supposed as constant in the following simulation. A_s is the effective area of solar sail, m_s is the total mass of solar sail. $\boldsymbol{n} = (\cos\alpha\cos(\omega_s\ t), -\cos\alpha\sin(\omega_s\ t), \sin\alpha)^{\mathrm{T}}$ is the normal vector of the solar sail, $\boldsymbol{l} = (\cos(\omega_s\ t), -\sin(\omega_s\ t), 0)^{\mathrm{T}}$ is the unit vector in the Sun line direction, α is the pitch angle between the norm of the sail and Sun line, ω_s is the invariable angular rate of the Sun line in the corotating frame in the dimensionless synodic coordinate system [27]. We consider such a scenario where two primaries are far away from the Sun that the annual changes in the inclination of the Sun line with respect to the plane of the system are too small to be considered and solar radiation pressure stays the same in this article.

B. Equations of motion

The RTBP with the larger primary an oblate spheroid is investigated. We use a barycentric, rotating and dimensionless coordinate system $Oxyz$; the origin is at the barycenter of the primaries; the axis x is along the line joining with the primaries; the direction of the orbital angular velocity ω of the smaller primary defines the axis z; and the axis y completes the right-handed triad. We describe the circular restricted three-body problem in Figure 2. For convenience the dimensionless form is often used [28]. The two primaries have masses m_1 and m_2 respectively, the mass of the infinitesimal body, the solar sail, is m_s. The distance between the primaries is $\left\|\overrightarrow{P_1P_2}\right\|$, and the gravitational constant is chosen to be unity. When it comes to the RTBP, the unit mass, length, and time of the system are defined as

$$\begin{aligned} [M] &= m_1 + m_2 \\ [L] &= \left\|\overrightarrow{P_1P_2}\right\| \\ [T] &= \sqrt{\left\|\overrightarrow{P_1P_2}\right\|^3 / G(m_1+m_2)} \end{aligned} \quad (2)$$

Then, in this system the masses of two primaries are $m_1 = 1-\mu, m_2 = \mu$, where μ is the mass ratio of the system, $\mu = m_2/(m_1+m_2)$.The distances of two primaries to the barycenter are $\left\|\overrightarrow{P_1O}\right\| = \mu, \left\|\overrightarrow{OP_2}\right\| = 1-\mu$.

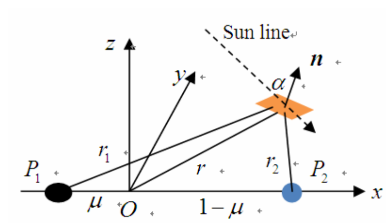

Figure 2. Schematic geometry of the circular restricted three-body problem in the solar system

Considering the oblateness of the larger primary, the equations of motion of the sail in the rotating coordinate system can be written as

$$\ddot{x} - 2n\dot{y} = \Omega_x + a_x \quad (3)$$

$$\ddot{y} + 2n\dot{x} = \Omega_y + a_y \quad (4)$$

$$\ddot{z} = \Omega_z + a_z \quad (5)$$

where Ω is the pseudo-potential function [22]

$$\Omega = \frac{n^2}{2}(x^2 + y^2) + \frac{1-\mu}{r_1} + \frac{\mu}{r_2} + \frac{(1-\mu)A_1}{2r_1^3} - \frac{3(1-\mu)A_1 z^2}{2r_1^5} \quad (6)$$

$\Omega_x, \Omega_y, \Omega_z$ are the components of the partial derivative of the pseudo-potential function Ω on each coordinate axis; $r_1 = \sqrt{(x+\mu)^2 + y^2 + z^2}$, $r_2 = \sqrt{(x+\mu-1)^2 + y^2 + z^2}$ are the distances of the solar sail from the primaries respectively, and $n = \sqrt{1 + 3A_1/2}$ is the perturbed mean motion of the primaries; $A_1 = (R_E{}^2 - R_P{}^2)/5R^2$ is the oblateness coefficient of the larger primary, where R_E and R_P are the equatorial and polar radii of the larger primary, and R is the distance between the two primaries [29]. a_x, a_y, a_z are the projections of the acceleration of solar radiation pressure on the axis Ox, Oy, Oz . $a_0 = PA_s / m_s$ is regarded as characteristic acceleration of the sail.

$$a_x = a_0 \cos\alpha \cos(\omega_s t)(\rho_r \cos 2\alpha + 1) \quad (7)$$

$$a_y = -a_0 \cos\alpha \sin(\omega_s t)(\rho_r \cos 2\alpha + 1) \quad (8)$$

$$a_z = a_0 \rho_r \cos\alpha \sin 2\alpha \quad (9)$$

III. COLLINEAR EQUILIBRIUM POINTS

The equilibrium points of the system are the solutions of the equations

$$\Omega_x + a_x = 0 \quad (10)$$

$$\Omega_y + a_y = 0 \quad (11)$$

$$\Omega_z + a_z = 0 \quad (12)$$

Where

$$\Omega_x = n^2 x - \frac{(1-\mu)(x+\mu)}{r_1^3} - \frac{\mu(x+\mu-1)}{r_2^3} - \frac{3A_1(1-\mu)(x+\mu)}{2r_1^5} + \frac{15A_1 z^2 (1-\mu)(x+\mu)}{2r_1^7} \quad (13)$$

$$\Omega_y = n^2 y - \frac{(1-\mu)y}{r_1^3} - \frac{\mu y}{r_2^3} - \frac{3A_1(1-\mu)y}{2r_1^5} + \frac{15A_1 z^2 (1-\mu)y}{2r_1^7} \quad (14)$$

$$\Omega_z = -\frac{(1-\mu)z}{r_1^3} - \frac{\mu z}{r_2^3} - \frac{9A_1(1-\mu)z}{2r_1^5} + \frac{15A_1(1-\mu)z^3}{2r_1^7} \quad (15)$$

It is well known that the restricted three-body problem has five Lagrange points, including three collinear equilibrium points and two triangular equilibrium points [28]. In this article we mainly discuss the collinear Lagrange points and displaced orbits in the neighborhood of these points. We suppose that three collinear equilibrium points $L_i (i = 1,2,3)$ lie on the axis x , then we use $\boldsymbol{r}_e = (x_e, 0, 0)^{\mathbf{T}}$ to denote the collinear equilibria. These collinear Lagrange points satisfy (10), (11) and (12), to give (16)

$$n^2 x - \frac{(1-\mu)(x+\mu)}{|x+\mu|^3} - \frac{\mu(x+\mu-1)}{|x+\mu-1|^3} - \frac{3A_1(1-\mu)(x+\mu)}{2|x+\mu|^5} + a_0(1+\rho_r) = 0 \quad (16)$$

and $\alpha = 0, \omega_s t = 2k\pi (k \in Z)$. From (16) we see that the positions of collinear equilibrium points vary with the magnitude of the oblateness coefficient A_1 and reflection coefficient ρ_r . Ariadna [25] has already presented the effects of reflection coefficient ρ_r on equilibrium points in Hill's three-body problem. In the following simulation, we consider variational oblateness with reflection coefficient ρ_r fixed, $\rho_r = 0.88$. Figure 3 shows the positions of the collinear points $L_i (i = 1,2,3)$ change as the value of the oblateness varies. It is clear that with the increasement of oblateness, L_1 and L_2 come close to the smaller primary, while L_3 goes far away from the primaries.

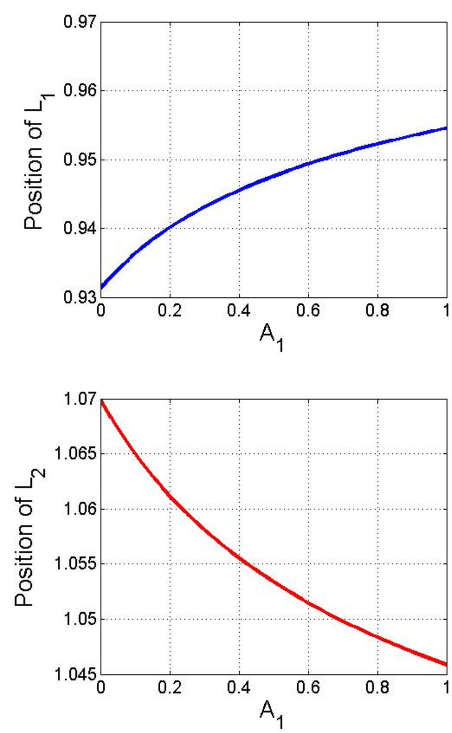

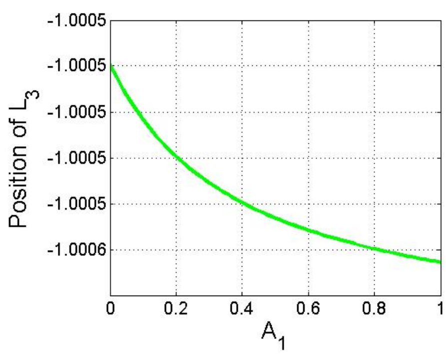

Figure 3. Positions of the collinear equilibrium points for different oblateness A_1 varying from zero to one with $\mu = 0.001$ and $a_0 = 0.0001$

IV. Linearization near the collinear equilibria

To further investigate the characteristics of the solar sail orbit, we need to linearize the system because the differential equations are nonlinear. Given that the collinear Lagrange points of the nonlinear system are $\boldsymbol{r}_e = (x_e, 0, 0)^{\mathbf{T}}$, we introduce small perturbations such that we define (17), (18), and (19)

$$x = x_e + \xi \quad (17)$$

$$y = \eta \quad (18)$$

$$z = \zeta \quad (19)$$

Substitute (17), (18), and (19) into (3), (4), (5), and assume that the sail acceleration is constant under the small perturbation from the collinear equilibrium point [30, 31]; then we obtain the variational equations

$$\ddot{\xi} - 2n\dot{\eta} = \Omega^e_{xx}\xi + u_\xi \quad (20)$$

$$\ddot{\eta} + 2n\dot{\xi} = \Omega^e_{yy}\eta + u_\eta \quad (21)$$

$$\ddot{\zeta} = \Omega^e_{zz}\zeta + u_\zeta \quad (22)$$

where

$$\Omega_{xx} = n^2 - \frac{1-\mu}{r_1^3} + \frac{3(1-\mu)(x+\mu)^2}{r_1^5} - \frac{\mu}{r_2^3} + \frac{3\mu(x+\mu-1)^2}{r_2^5} - \frac{3A_1(1-\mu)}{2r_1^5} + \frac{15A_1(1-\mu)(x+\mu)^2}{2r_1^7} + \frac{15A_1z^2(1-\mu)}{2r_1^7} - \frac{105A_1z^2(1-\mu)(x+\mu)^2}{2r_1^9} \quad (23)$$

$$\Omega_{yy} = n^2 - \frac{1-\mu}{r_1^3} + \frac{3(1-\mu)y^2}{r_1^5} - \frac{\mu}{r_2^3} + \frac{3\mu y^2}{r_2^5} - \frac{3A_1(1-\mu)}{2r_1^5} + \frac{15A_1(1-\mu)y^2}{2r_1^7} + \frac{15A_1z^2(1-\mu)}{2r_1^7} - \frac{105A_1z^2(1-\mu)y^2}{2r_1^9} \quad (24)$$

$$\Omega_{zz} = -\frac{1-\mu}{r_1^3} + \frac{3(1-\mu)z^2}{r_1^5} - \frac{\mu}{r_2^3} + \frac{3\mu z^2}{r_2^5} - \frac{9A_1(1-\mu)}{2r_1^5} + \frac{90A_1(1-\mu)z^2}{2r_1^7} - \frac{105A_1z^4(1-\mu)}{2r_1^9} \quad (25)$$

$$\boldsymbol{u} = \begin{bmatrix} u_\xi \\ u_\eta \\ u_\zeta \end{bmatrix} = \begin{bmatrix} a_0\cos\alpha\cos(\omega_s\,\mathrm{t})(\rho_r\cos 2\alpha + 1) \\ -a_0\cos\alpha\sin(\omega_s\,\mathrm{t})(\rho_r\cos 2\alpha + 1) \\ a_0\rho_r\cos\alpha\sin 2\alpha \end{bmatrix} \quad (26)$$

Therein $\Omega^e_{ij}(i, j = x, y, z)$ is the evaluation of the second order partial derivative of the potential function at the equilibrium points. With this method we can get the linear dynamic model and establish its state-space equation expressed in matrix notaion as

$$\dot{\mathbf{X}} = \mathbf{AX} + \mathbf{Bu} \quad (27)$$

where the six-dimensional state vector is defined $\mathbf{X} = (\xi, \eta, \zeta, \dot{\xi}, \dot{\eta}, \dot{\zeta})^{\mathrm{T}}$, and

$$\mathbf{A} = \begin{pmatrix} 0 & 0 & 0 & 1 & 0 & 0 \\ 0 & 0 & 0 & 0 & 1 & 0 \\ 0 & 0 & 0 & 0 & 0 & 1 \\ \Omega^e_{xx} & 0 & 0 & 0 & 2n & 0 \\ 0 & \Omega^e_{yy} & 0 & -2n & 0 & 0 \\ 0 & 0 & \Omega^e_{zz} & 0 & 0 & 0 \end{pmatrix}, \mathbf{B} = \begin{pmatrix} 0 & 0 & 0 \\ 0 & 0 & 0 \\ 0 & 0 & 0 \\ 1 & 0 & 0 \\ 0 & 1 & 0 \\ 0 & 0 & 1 \end{pmatrix},$$

$$\mathbf{u} = (u_\xi, u_\eta, u_\zeta)^{\mathbf{T}} \quad (28)$$

V. Simulations

A. Tracking reference orbit

In this section, we choose a particular periodic orbit above the ecliptic plane as a reference orbit like Farquhar [32] and Simo [27] did

$$\xi_{ref} = \xi_0\cos(\omega_s t) \quad (29)$$

$$\eta_{ref} = \eta_0\sin(\omega_s t) \quad (30)$$

$$\zeta_{ref} = \zeta_0 \quad (31)$$

then substitute (29), (30), (31) into the variational equations (20 ~ 22), we will get

$$\xi_0 = -\frac{(\omega_s^2 + 2n\omega_s + b)d}{ab - 4n^2\omega_s^2 + a\omega_s^2 + b\omega_s^2 + \omega_s^4} \quad (32)$$

$$\eta_0 = \frac{(\omega_s^2 + 2n\omega_s + a)d}{ab - 4n^2\omega_s^2 + a\omega_s^2 + b\omega_s^2 + \omega_s^4} \quad (33)$$

$$\zeta_0 = -\frac{a_0\rho_r \cos\alpha \sin 2\alpha}{c} \quad (34)$$

where $a = \Omega_{xx}^e$, $b = \Omega_{yy}^e$, $c = \Omega_{zz}^e$, $d = a_0 \cos\alpha(\rho_r \cos 2\alpha + 1)$. From (34), solar sail will reach maximum displacement above the ecliptic plane when the pitch angle approximately equals 0.615*rad* or 35.264^0, which is consistent with Simo [27].

The LQR controller is developed to stabilize the displaced orbit in the neighborhood of the collinear libration point to track the reference orbit $\mathbf{X}_{ref} = (\xi_{ref}, \eta_{ref}, \zeta_{ref})^{\mathbf{T}}$. Then we will set $\Delta\mathbf{X} = \mathbf{X} - \mathbf{X}_{ref}$ and apply a linear feedback control $\Delta\boldsymbol{u} = \mathbf{u} - \mathbf{u}_{ref} = -\mathbf{K}(\mathbf{X} - \mathbf{X}_{ref})$ to (27) that minimizes the quadratic cost function

$$\min J = \frac{1}{2}\int_0^\infty [\Delta\mathbf{X}^{\mathbf{T}}\mathbf{Q}\Delta\mathbf{X} + \Delta\mathbf{u}^{\mathbf{T}}\mathbf{R}\Delta\mathbf{u})dt \quad (35)$$

where the matrices $\mathbf{Q}$ and $\mathbf{R}$ represent the weights of the state and control, which are symmetric positive semidefinite and free to be chosen. We obtain the gain matrix $\mathbf{K} = \mathbf{R}^{-1}\mathbf{B}^{\mathbf{T}}\mathbf{P}$ by solving the algebraic Riccati equation [33]

$$\mathbf{A}^{\mathbf{T}}\mathbf{P} + \mathbf{P}\mathbf{A} - \mathbf{P}\mathbf{B}\mathbf{R}^{-1}\mathbf{B}^{\mathbf{T}}\mathbf{P} + \mathbf{Q} = \mathbf{0} \quad (36)$$

then the closed-loop system is obtained as

$$\Delta\dot{\mathbf{X}} = (\mathbf{A} - \mathbf{BK})\Delta\mathbf{X} \quad (37)$$

A necessary and sufficient condition for the collinear equilibrium points to be linearly stable is that the real part of the eigenvalues of the matrix $\mathbf{A} - \mathbf{BK}$ are all less than or equal to zero [34].

B. Results

Initial conditions and parameters of system for simulation are elaborated in TABLE I.

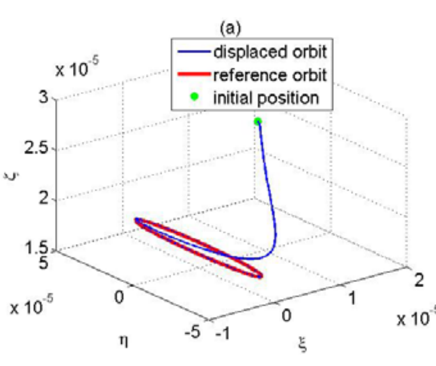

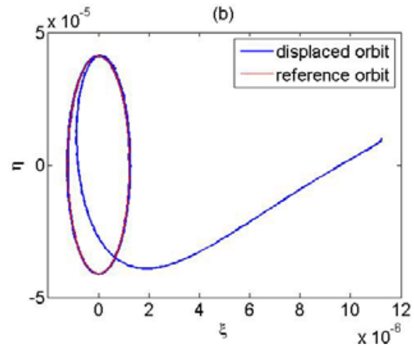

Figure 4. (a): Asymptotically stable periodic displaced orbit for solar sail near L_2 tracking the reference orbit (b): The projection of displaced orbits and the reference orbit on $\xi-\eta$ plane

By means of tracking the reference orbit, an asymptotically periodic displaced orbit is presented in Figure 4 (a). Figure 4 (b) is the projection of displaced orbits and the reference orbit on $\xi\eta$ plane, where it is clearly display the movement from initial disturbance point to the reference orbit. From Figure 5, we can find that the acceleration due to solar radiation pressure swings back and forth on axis ξ and η. However, the acceleration of solar sail on axis ζ fluctuates irregularly in the initial part of time, after that it becomes stable and turns to be constant. It means that the pitch angle of solar sail will remain unchanged eventually. Figure 6 is a very good explanation. We can obtain the numerical solutions of the pitch angle of solar sail by solve (26). After a period of time, the fluctuation disappears and pitch angle of solar sail stabilizes at 45°.

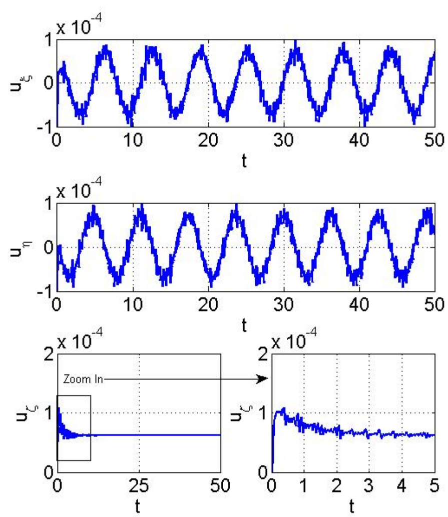

Figure 5. Solar radiation pressure acceleration projected on $\xi\eta\zeta$ axis

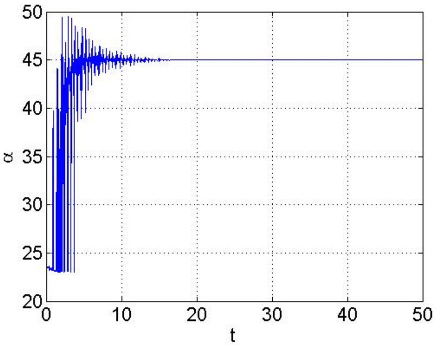

Figure 6 Pitch angle of solar sail vs time

State matrix $\mathbf{A}$ has two pairs of pure imaginary eigenvalues, $\pm 1.98668775i$ and $\pm 1.91578826i$, also a couple of real eigenvalues, ± 2.36689097. In the sense of Lyapunov[35], the system (27) is unstable. By using LQR, the new closed-loop system is stable, whose eigenvalues have all negative real parts. Select different initial conditions, $\mathbf{Q}$ or $\mathbf{R}$ will get different solar sail orbit for different space mission. Figure 7 is an example of solar sail quasi-periodic orbit, which is asymptotically stable.

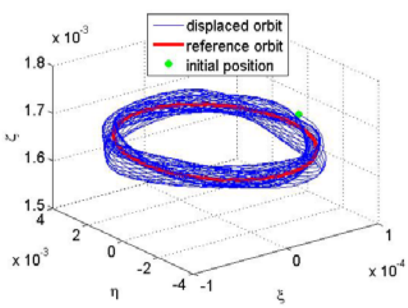

Figure 7. Quasi-periodic displaced orbit for solar sail

TABLE I. PARAMETERS OF SYSTEM AND INITIAL CONDITIONS FOR SIMULATION

Parameters	value
Mass ratio	0.001
Oblateness	0.005
Angular rate of the Sun line	0.9958
Characteristic acceleration	0.0001
Initial conditions	$[10^{-5};10^{-5};10^{-5};0;0;0]$
Position of L_2	1.069612985661655
Matrix $\mathbf{Q}$	$diag([10^3,10^3,10^3,10^3,10^3,10^3])$
Matrix $\mathbf{R}$	$diag([1,1,1])$
Pitch angle of reference orbit	$\pi/4$

VI. CONCLUSIONS

In this paper we investigate the solar sail displaced orbits in the circular restricted three-body problem with oblateness. We found that oblateness has some impact on the position of the collinear equilibrium point. An LQR controller is used to obtain the numerical solution of the components of solar radiation pressure acceleration. We solve (26) to get the changing laws of the pitch angle of the sail, which can make the system stable. Periodic and quasi-periodic displaced orbit could implement long-term observation arrangement.

REFERENCES

[1] E. Morrow, D. J. Scheeres, and D. Lubin, "Solar sail orbit operations at asteroids," *Journal of Spacecraft and Rockets*, vol. 38, pp. 279-286, Mar-Apr 2001.

[2] M. Leipold, M. Eiden, C. Gamer, L. Herbeck, D. Kassing, T. Niederstadt, *et al.*, "Solar sail technology development and demonstration," *Acta Astronautica*, vol. 52, pp. 317-326, JAN-MAR 2003 2003.

[3] H. Baoyin and C. R. McInnes, "Solar Sail Equilibria in the Elliptical Restricted Three-Body Problem," *Journal of Guidance, Control, and Dynamics*, vol. 29, pp. 538-543, 2006/05/01 2004.

[4] J. D. Biggs, C. R. McInnes, and T. Waters, "Control of Solar Sail Periodic Orbits in the Elliptic Three-Body Problem," *Journal of Guidance, Control, and Dynamics*, vol. 32, pp. 318-320, 2009/01/01 2005.

[5] J. Simo and C. R. Mclnnest, "Displaced Solar Sail Orbits: Dynamics and Applications," *Spaceflight Mechanics 2010, Pts I-Iii*, vol. 136, pp. 1803-1816, 2010 2010.

[6] C. R. McInnes, *Solar Sailing: Technology, Dynamics and Mission Applications*. London: Springer Praxis, 1999.

[7] Y. Tsuda, O. Mori, R. Funase, H. Sawada, T. Yamamoto, T. Saiki, *et al.*, "Flight status of IKAROS deep space solar sail demonstrator," *Acta Astronautica*, vol. 69, pp. 833-840, NOV-DEC 2011 2011.

[8] L. Johnson, M. Whorton, A. Heaton, R. Pinson, G. Laue, and C. Adams, "NanoSail-D: A solar sail demonstration mission," *Acta Astronautica*, vol. 68, pp. 571-575, MAR-APR 2011 2011.

[9] V. Lappas, N. Adeli, L. Visagie, J. Fernandez, T. Theodorou, W. Steyn, *et al.*, "CubeSail: A low cost CubeSat based solar sail demonstration mission," *Advances in Space Research*, vol. 48, pp. 1890-1901, DEC 1 2011 2011.

[10] R. S. Olive and L. Vaios, "Deorbitsail: a deployable sail for de-orbiting," in *54th AIAA/ASME/ASCE/AHS/ASC Structures, Structural Dynamics, and Materials Conference*, ed: American Institute of Aeronautics and Astronautics, 2013.

[11] H. Jeannette, D. Ben, D. William, and M. Colin, "Sunjammer: Preliminary End-to-End Mission Design," presented at the AIAA/AAS Astrodynamics Specialist

Conference, 2014.

[12] J. Simo and C. R. Mcinnes, "Displaced Periodic Orbits with Low-Thrust Propulsion in the Earth-Moon System," in *Aas/aiaa Space Flight Mechanics Meeting*, 2009.

[13] S. Gong, H. Baoyin, and J. Li, "Coupled attitude–orbit dynamics and control for displaced solar orbits," *Acta Astronautica*, vol. 65, pp. 730-737, 2009.

[14] C. McInnes, "Displaced non-Keplerian orbits using impulsive thrust," *Celestial Mechanics & Dynamical Astronomy*, vol. 110, pp. 199-215, JUL 2011 2011.

[15] M. Ceriotti and C. R. Mcinnes, "Natural and sail-displaced doubly-symmetric Lagrange point orbits for polar coverage," *Celestial Mechanics & Dynamical Astronomy*, vol. 114, pp. 151-180, 2012.

[16] H. Baoyin and C. R. McInnes, "Solar sail equilibria in the elliptical restricted three-body problem," *Journal of Guidance Control and Dynamics*, vol. 29, pp. 538-543, May-Jun 2006.

[17] P. Verrier, T. Waters, and J. Sieber, "Evolution of the L1 halo family in the radial solar sail circular restricted three-body problem," *Celestial Mechanics & Dynamical Astronomy*, vol. 120, pp. 373-400, Dec 2014.

[18] R. K. Sharma and P. V. S. Rao, "Stationary solutions and their characteristic exponents in the restricted three-body problem when the more massive primary is an oblate spheroid," *Celestial Mechanics & Dynamical Astronomy*, vol. 13, pp. 137-149, 1976.

[19] R. K. Sharma, "Periodic Orbits of 1st Kind in Restricted 3-Body Problem When More Massive Primary Is an Oblate Spheroid," *Astronomy & Astrophysics*, vol. 50, pp. 257-258, 1976.

[20] R. K. Sharma, "Periodic-Orbits of the 3rd Kind in the Restricted 3-Body Problem with Oblateness," *Astrophysics and Space Science*, vol. 166, pp. 211-218, Apr 1990.

[21] M. P. Markakis, A. E. Perdiou, and C. N. Douskos, "The photogravitational Hill problem with oblateness: equilibrium points and Lyapunov families," *Astrophysics and Space Science*, vol. 315, pp. 297-306, Jun 2008.

[22] C. Douskos and V. Markellos, "Out-of-plane equilibrium points in the restricted three-body problem with oblateness," *Astronomy & Astrophysics*, vol. 446, pp. 357-360, JAN 2006 2006.

[23] J. Singh, "Combined Effects of Oblateness and Radiation on the Nonlinear Stability of L4in the Restricted Three-Body Problem," *The Astronomical Journal*, vol. 137, pp. 3286-3292, 2009.

[24] J. L. Wright, "Space Sailing," *Physics Today*, vol. 45, 1992.

[25] A. Farrés, À. Jorba, J. M. Mondelo, and B. Villac, "Periodic Motion for an Imperfect Solar Sail Near an Asteroid," presented at the International Symposium on Solar Sailing, 2013.

[26] B. Dachwald, V. Baturkin, V. L. Coverstone, B. Diedrich, G. P. Garbe, M. Gorlichk, *et al.*, "Potential effects of optical solar sail degredation on trajectory design," *Advances in the Astronautical Sciences*, vol. 123, 2005.

[27] J. Simo and C. McInnes, "Solar sail orbits at the Earth-Moon libration points," *Communications in Nonlinear Science and Numerical Simulation*, vol. 14, pp. 4191-4196, DEC 2009 2009.

[28] V. Szebehely, *Theory of orbits: the restricted problem of three bodies*. New York: London:Academic Press, 1967.

[29] R. K. Sharma and P. V. S. Rao, "A case of Commensurability Induced by Oblateness," *Celestial Mechanics*, vol. 18, pp. 185-194, 1978 1978.

[30] J. Simo and C. R. McInnes, "Solar sail orbits at the Earth-Moon libration points," *Communications in Nonlinear Science and Numerical Simulation*, vol. 14, pp. 4191-4196, Dec 2009.

[31] S. P. Gong, J. F. Li, and J. Simo, "Orbital Motions of a Solar Sail Around the L2 Earth-Moon Libration Point," *Journal of Guidance Control and Dynamics*, vol. 37, pp. 1349-1356, Jul-Aug 2014.

[32] R. W. Farquhar, "The control and use of libration-point satellites," *Dissertations & Theses*, 1970.

[33] B. Wie, *Space Vehicle Dynamics and Control*: AIAA, 1998.

[34] J. D. Biggs and C. R. Mcinnes, "Passive Orbit Control for Space-Based Geo Engineering," *Journal of Guidance Control & Dynamics*, vol. 33, pp. 1017-1020, 2010.

[35] A. M. LYAPUNOV, "The general problem of the stability of motion," *Journal of Applied Mechanics*, vol. 31, pp. 353-354, 1995.